

DESY 04-042
 TTP04-06
 UB-ECM-PF-04-05

$M(B_c^*) - M(B_c)$ Splitting from Nonrelativistic Renormalization Group

A.A. Penin^{a,b}, A. Pineda^c, V.A. Smirnov^{d,e}, M. Steinhauser^e

^a *Institut für Theoretische Teilchenphysik, Universität Karlsruhe, 76128 Karlsruhe, Germany*

^b *Institute for Nuclear Research, Russian Academy of Sciences, 117312 Moscow, Russia*

^c *Dept. d'Estructura i Constituents de la Matèria, U. Barcelona, E-08028 Barcelona, Spain*

^d *Institute for Nuclear Physics, Moscow State University, 119992 Moscow, Russia*

^e *II. Institut für Theoretische Physik, Universität Hamburg, 22761 Hamburg, Germany*

Abstract

We compute the hyperfine splitting in a heavy quarkonium composed of different flavors in next-to-leading logarithmic approximation using the nonrelativistic renormalization group. We predict the mass difference of the vector and pseudoscalar charm-bottom mesons to be $M(B_c^*) - M(B_c) = 48 \pm 15 \text{ (th)}^{+14}_{-11} (\delta\alpha_s) \text{ MeV}$.

PACS numbers: 12.38.Bx, 14.65.Fy, 14.65.Ha

1 Introduction

The recently discovered charm-bottom heavy quarkonium completes the well investigated charmonium and bottomonium families and offers a new perspective in the study of the nonrelativistic dynamics of the strong interactions. The first experimental observation of about twenty events interpreted as the decays of the B_c meson by CDF collaboration [1] does not match the precision of the spin one charmonium and bottomonium measurements. The statistics, however, is expected to increase significantly in future experiments at Tevatron and LHC greatly improving the accuracy of the data. Note that only the pseudoscalar (spin singlet) state has been observed so far while the vector (spin triplet) meson B_c^* is still to be discovered. This distinguishes $c\bar{b}$ quarkonium from the $b\bar{b}$ system, where it is the pseudoscalar η_b meson, which asks for experimental detection.

From the theoretical point of view, the charm-bottom mesons are “in between” the approximately Coulomb $b\bar{b}$ mesons and the $c\bar{c}$ mesons. Therefore, a simultaneous analysis of all three quarkonia could shed new light on the balance between the perturbative and nonperturbative effects and further check whether a perturbative analysis provides a reliable starting point for them. Moreover, since the nonperturbative effects in the $c\bar{b}$ system are suppressed with respect to the $c\bar{c}$ meson, the former could be a cleaner place to determine

the charm quark mass (provided the experimental accuracy is good enough). Another point to be stressed is that, though the leading order dynamics of the $c\bar{b}$ state is quite similar to the $b\bar{b}$ and $c\bar{c}$ one (up to the value of the reduced mass) the higher order relativistic and perturbative corrections are different. Thus the comparison of $c\bar{b}$ and $b\bar{b}$ ($c\bar{c}$) properties could help to establish fine details of the nonrelativistic dynamics.

The spectrum of the charm-bottom quarkonium has been subject of numerous investigations based on potential models [2, 3], lattice simulations [4], and pNRQCD [5]. This last analysis computed the ground state energy within a pure perturbative approach. We consider that this analysis further indicates that a perturbative approach can be a good starting point for studying the B_c system.

In the present paper we focus on the hyperfine splitting (HFS) E_{hfs} of the B_c , *i.e.* the mass difference between the singlet and triplet spin states $M(B_c^*) - M(B_c)$. The QCD study of the heavy quarkonium HFS has a long history [6, 7]. For the same-flavor quarkonium the next-to-leading order (NLO) $\mathcal{O}(\alpha_s)$ correction to the ground state HFS can be found in [8] in a closed analytical form. The leading order HFS is proportional to the fourth power of the strong coupling constant $\alpha_s(\nu)$ and thus the low order calculations suffer from strong spurious dependence on the renormalization scale ν , which essentially limits the numerical accuracy of the approximation. Hence, the proper fixing of the normalization scale becomes mandatory for the HFS phenomenology. The dynamics of the nonrelativistic bound state, however, is characterized by three well separated scales: the hard scale of the heavy quark mass m , the soft scale of the bound state momentum mv , and the ultrasoft scale of the bound state energy mv^2 , where $v \propto \alpha_s$ is the velocity of the heavy quark inside the approximately Coulomb bound state. To make the procedure of scale fixing self-consistent one has to resum to all orders the large logarithms of the scale ratios. For the same-flavor case this problem has been solved in Ref. [9] within the nonrelativistic renormalization group (NRG) approach and the next-to-leading logarithmic (NLL) result for HFS has been derived. The renormalization group improved result shows better stability with respect to the scale variation. Moreover, the use of the NRG significantly improves the agreement with the experimental value of HFS in charmonium in comparison to the NLO computation. Below we generalize the analysis to the different-flavor quarkonium case and apply the result to predict the splitting $M(B_c^*) - M(B_c)$.

2 Renormalization group running of the spin dependent potential

To derive the NRG equations necessary for the NLL analysis of the HFS, we rely on the method based on the formulation of the nonrelativistic effective theory [10] known as potential NRQCD (pNRQCD) [11]. The method was developed in Ref. [12] where, in particular, the leading logarithmic (LL) result for HFS has been obtained (see also Ref. [13]). In pNRQCD the HFS is generated by the spin-flip potential in the effective Hamiltonian, which

in momentum space has the form

$$\delta\mathcal{H}_{\text{spin}} = D_{S^2,s}^{(2)} \frac{4C_F\pi}{3m_1m_2} \mathbf{S}^2, \quad \mathbf{S} = \frac{\boldsymbol{\sigma}_1 + \boldsymbol{\sigma}_2}{2}, \quad (1)$$

where $\boldsymbol{\sigma}_1$ and $\boldsymbol{\sigma}_2$ are the spin operators of the quark and antiquark with masses m_1 and m_2 , $C_F = (N_c^2 - 1)/(2N_c)$, and $D_{S^2,s}^{(2)}$ is the Wilson coefficient, which incorporates the effects of the modes that have been integrated out. In effective theory calculations such couplings become singular as a result of the scale separation. The renormalization of these singularities allows one to derive the equations of the NRG, which describe the running of the effective-theory couplings, *i.e.* their dependence on the effective-theory cutoffs. The solution of these equations sums up the logarithms of the scale ratios.

In general, one should consider the soft, potential and ultrasoft running of $D_{S^2,s}^{(2)}$ corresponding to the ultraviolet divergences of the soft, potential, and ultrasoft regions [14]. We denote the corresponding cutoffs as ν_s , ν_p and ν_{us} , respectively. ν_{us} and ν_p are correlated as was first realized in Ref. [15]. A natural relation between them is $\nu_{us} = \nu_p^2/(2m_r)$, where $m_r = m_1m_2/(m_1 + m_2)$ is the reduced mass. The dependence on ν_s first emerges in the LL approximation after integrating out the hard modes. It disappears after subsequent integrating out the soft modes giving rise to a dependence on k , the three-dimensional momentum transfer between the quark and antiquark. Thus the soft running effectively stops at $\nu_s = k$. The dependence on ν_p emerges for the first time in the NLL approximation and cancels out in the time-independent Schrödinger perturbation theory for heavy quarkonium observables. Thus, in pNRQCD one considers $D_{S^2,s}^{(2)}$ as a function of k and ν_p . For the calculation of the spectrum it is convenient to expand this k -dependent potential around $k = \nu_s$

$$D_{S^2,s}^{(2)}(k, \nu_p) = D_{S^2,s}^{(2)}(\nu_s, \nu_p) + \ln\left(\frac{k}{\nu_s}\right) \nu_s \frac{d}{d\nu_s} D_{S^2,s}^{(2)}(\nu_s, \nu_p) + \dots \quad (2)$$

The characteristic momentum for the Coulomb system is $\alpha_s m_r$ and for $\nu_s \sim \alpha_s m_r$ the average of $\ln(k/\nu_s)$ over bound state wave function does not produce a large logarithm while the derivative in $\ln \nu_s$ results in extra factor of α_s . Thus, for the calculation of the HFS in NLL approximation one can take the first term on the right hand side of Eq. (2) in the NLL approximation, the second term in the LL approximation and neglect the higher derivative terms.

Once expanded, the potential is a function of ν_s and ν_p (we should not forget that there is also a dependence on m_i , the masses of the heavy quarks, and ν_h , the matching scale of the order of the heavy quark masses). Let us start with the discussion of the soft running. To the NLL approximation it is determined by the following NRG equation

$$\nu_s \frac{d}{d\nu_s} D_{S^2,s}^{(2)} = \alpha_s c_F(m_1) c_F(m_2) \gamma_s, \quad (3)$$

where c_F is the effective Fermi coupling,

$$\gamma_s = \gamma_s^{(1)} \frac{\alpha_s}{\pi} + \gamma_s^{(2)} \frac{\alpha_s^2}{\pi^2} + \dots \quad (4)$$

is the soft anomalous dimension and $\alpha_s = \alpha_s(\nu_s)$ is renormalized in the $\overline{\text{MS}}$ scheme. The running of the coefficient c_F is known in NLL approximation [16]. It reads

$$c_F(m_i) = z^{-\frac{\gamma_0}{2}} \left[1 + \frac{\alpha_s(\nu_h)}{4\pi} \left(c_1 + \frac{\gamma_0}{2} \ln \frac{\nu_h^2}{m_i^2} \right) + \frac{\alpha_s(\nu_h) - \alpha_s(\nu_s)}{4\pi} \left(\frac{\gamma_1}{2\beta_0} - \frac{\gamma_0\beta_1}{2\beta_0^2} \right) + \dots \right], \quad (5)$$

where $z = (\alpha_s(\nu_s)/\alpha_s(\nu_h))^{1/\beta_0}$, $\nu_h \sim m_i$ is the hard matching scale, $c_1 = 2(C_A + C_F)$ and the one- and two-loop anomalous dimensions read [16]

$$\gamma_0 = 2C_A, \quad \gamma_1 = \frac{68}{9}C_A^2 - \frac{52}{9}C_A T_F n_l. \quad (6)$$

Here $C_A = N_c$, $T_F = 1/2$, n_l is the number of massless quark flavors, and β_i is the $(i+1)$ -loop coefficient of the QCD β function

$$\beta_0 = \frac{11}{3}C_A - \frac{4}{3}T_F n_l, \quad \beta_1 = \frac{34}{3}C_A^2 - \frac{20}{3}C_A T_F n_l - 4C_F T_F n_l. \quad (7)$$

The value of one-loop anomalous dimension

$$\gamma_s^{(1)} = -\frac{\beta_0}{2} + \frac{7}{4}C_A \quad (8)$$

can be extracted from the result of Ref. [12]. The result for the two-loop coefficient

$$\gamma_s^{(2)} = \frac{1}{216} \left[C_A^2 (5 - 36\pi^2) + 88C_A n_l T_F + 4n_l T_F (27C_F - 40n_l T_F) \right], \quad (9)$$

is new. It was obtained by an explicit calculation of the subleading singularities of the two-loop soft diagrams using the approach of [17, 18, 19]. In this approach, dimensional regularization with $D = 4 - 2\epsilon$ is used to handle the divergences, and the formal expressions derived from the Feynman rules of the effective theory are understood in the sense of the threshold expansion [14]. Thus the practical calculation reduces to the evaluation of the coefficients of the quadratic and linear soft poles in ϵ . Our approach possesses two crucial virtues: the absence of additional regulator scales and the automatic matching of the contributions from different scales. For the reduction of the two-loop Feynman integrals to the master ones the method of Ref. [20] was used.

The solution of Eq. (3) can be written as a sum of the LL and NLL contributions. The LL result is already known and reads [12] (see also [13])

$$\left(D_{S^2,s}^{(2)} \right)^{LL} = \alpha_s(\nu_h) \left[1 + \frac{2\beta_0 - 7C_A}{2\beta_0 - 4C_A} (z^{-2C_A + \beta_0} - 1) \right]. \quad (10)$$

For the NLL term we obtain

$$\left(\delta D_{S^2,s}^{(2)} \right)_s^{NLL} = B_1 \alpha_s^2(\nu_h) (z^{-\gamma_0 + \beta_0} - 1) + B_2 \alpha_s^2(\nu_h) (z^{-\gamma_0 + 2\beta_0} - 1), \quad (11)$$

where

$$B_1 = \frac{\beta_1 \gamma_0 - 2\beta_0^2 \left[c_1 + \frac{\gamma_0}{2} \ln \left(\frac{\nu_h^2}{m_1 m_2} \right) \right] - \beta_0 \gamma_1}{2\beta_0^2 (\beta_0 - \gamma_0) \pi} \gamma_s^{(1)}, \quad (12)$$

$$B_2 = \frac{-\beta_1 \gamma_0 \gamma_s^{(1)} + \beta_0 \gamma_1 \gamma_s^{(1)} + \beta_0 \left(\beta_1 \gamma_s^{(1)} - 4 \beta_0 \gamma_s^{(2)} \right)}{2\beta_0^2 (2\beta_0 - \gamma_0) \pi}. \quad (13)$$

The potential running starts to contribute in NLL order. To compute it we inspect all operators that lead to spin-dependent ultraviolet divergences in the time-independent perturbation theory contribution with one and two potential loops [12, 21, 22]. They are

- (i) the $\mathcal{O}(v^2, \alpha_s v)$ operators [6],
- (ii) the tree $\mathcal{O}(v^4)$ operators, some of which can be checked against the QED analysis [18, 23],
- (iii) the one-loop $\mathcal{O}(\alpha_s v^3)$ operators for which only the Abelian parts are known [18], while the non-Abelian parts are new.

In the NLL approximation, we need the LL soft and ultrasoft running of the $\mathcal{O}(v^2)$ and $\mathcal{O}(v^4)$ operators, which enter the two-loop time-independent perturbation theory diagrams, and the NLL soft and ultrasoft running of the $\mathcal{O}(\alpha_s v)$ and $\mathcal{O}(\alpha_s v^3)$ operators, which contribute at one loop. The running of the $\mathcal{O}(v^2, \alpha_s v)$ operators is already known within pNRQCD [12]. The running of the other operators is new. For some of them, it can be obtained using the reparameterization invariance [24]. We refrain from writing the corresponding system of NRG equations, which is rather lengthy, and only present its solution, which can be cast in the form

$$\left(\delta D_{S^2,s}^{(2)} \right)_p^{NLL} = \pi \alpha_s^2(\nu_h) \sum_{i=1}^{18} A_i f_i, \quad (14)$$

where the coefficients A_i and f_i are given in the Appendix. To get this result we rescale the ultrasoft cutoff to $\nu_{us} = \nu_p^2/\nu_h$. The difference to the previous definition is beyond the NLL accuracy.

The LL result (10) obeys the tree level matching condition

$$\left. \left(D_{S^2,s}^{(2)} \right)^{LL} \right|_{\nu=\nu_h} = \alpha_s(\nu_h), \quad (15)$$

while Eqs. (11) and (14) vanish at $\nu = \nu_h$ by construction. We then use the known one-loop result of the potential [6] to obtain the NLO matching condition at the scale $k = \nu_s = \nu_p = \nu_h$. It reads

$$\begin{aligned} \left(D_{S^2,s}^{(2)} \right)_{1\text{-loop}} &= \left[-\frac{5}{9} T_F n_l - \frac{5}{36} C_A + C_F + \frac{7}{8} C_A \ln \left(\frac{\nu_h^2}{m_1 m_2} \right) \right. \\ &\quad \left. - \frac{3}{4} \left(C_F \frac{m_1 - m_2}{m_1 + m_2} + \frac{1}{2} (C_A - 2C_F) \frac{m_1 + m_2}{m_1 - m_2} \right) \ln \left(\frac{m_2}{m_1} \right) \right] \frac{\alpha_s^2(\nu_h)}{\pi}. \end{aligned} \quad (16)$$

Note that in the limit $m_1 = m_2 \equiv m_q$ this equation does not reproduce the same-flavor equal-mass expression

$$\left(D_{S^2,s}^{(2)}\right)_{1\text{-loop}}^{q\bar{q}} = \left[-\frac{5}{9}T_F n_l + \frac{3}{2}(1 - \ln 2)T_F + \frac{11C_A - 9C_F}{18} + \frac{7}{4}C_A \ln \frac{\nu_h}{m_q}\right] \frac{\alpha_s^2(\nu_h)}{\pi}, \quad (17)$$

because of the two-gluon annihilation contribution present in the latter case.

Thus the NLL approximation for the Wilson coefficient is given by the sum

$$\left(D_{S^2,s}^{(2)}(\nu)\right)^{NLL} = \left(D_{S^2,s}^{(2)}(\nu)\right)^{LL} + \left(\delta D_{S^2,s}^{(2)}(\nu)\right)_s^{NLL} + \left(\delta D_{S^2,s}^{(2)}(\nu)\right)_p^{NLL} + \left(D_{S^2,s}^{(2)}\right)_{1\text{-loop}}. \quad (18)$$

where $D_{S^2,s}^{(2)}(\nu) \equiv D_{S^2,s}^{(2)}(\nu, \nu)$ and we combine the soft and potential running by setting $\nu_s = \nu_p = \nu$, which is consistent at the order of interest. From Eqs. (1) and (2) we obtain the final result for the NLL spin-flip potential

$$\delta\mathcal{H}_{\text{spin}} = \left[\left(D_{S^2,s}^{(2)}(\nu)\right)^{NLL} + \frac{\gamma_s^{(1)}}{\pi} \left(\alpha_s^2 c_F^2\right)^{LL} \ln\left(\frac{k}{\nu}\right)\right] \frac{4C_F\pi}{3m_1m_2} \mathbf{S}^2. \quad (19)$$

3 Hyperfine splitting in NLL approximation

We are now in the position to derive the NLL result for the HFS. It is obtained by computing the corrections to the energy levels with the insertion of the potential (19) in the quantum mechanical perturbation theory. The result for principal quantum number n reads

$$\begin{aligned} E_{n,\text{hfs}}^{NLL} = & -\frac{16}{3} \frac{C_F^2 \alpha_s^2}{n} \frac{m_r^2}{m_1 m_2} E_n^C \left\{ (1 + 2\delta\phi_n) \left(D_{S^2,s}^{(2)}(\nu)\right)^{LL} \right. \\ & + \left(-\ln\left(\frac{n\nu}{\bar{\nu}}\right) + \Psi_1(n+1) + \gamma_E + \frac{n-1}{2n} \right) \frac{\gamma_s^{(1)}}{\pi} \left(\alpha_s^2 c_F^2\right)^{LL} \\ & \left. + \left(\delta D_{S^2,s}^{(2)}(\nu)\right)_s^{NLL} + \left(\delta D_{S^2,s}^{(2)}(\nu)\right)_p^{NLL} + \left(D_{S^2,s}^{(2)}\right)_{1\text{-loop}}^{NLL} \right\}, \end{aligned} \quad (20)$$

where $\bar{\nu} = 2C_F\alpha_s m_r$, $E_n^C = -C_F^2 \alpha_s^2 m_r / (2n^2)$, $\Psi_n(z) = d^n \ln \Gamma(z) / dz^n$, $\Gamma(z)$ is the Euler Γ -function, and $\gamma_E = 0.577216\dots$ is Euler's constant. In Eq. (20) the first order correction to the Coulomb wave function at the origin due to one-loop contribution to the static potential reads [25]

$$\delta\phi_n = \frac{\alpha_s}{\pi} \left[\frac{3}{8} a_1 + \frac{\beta_0}{4} \left(3 \ln\left(\frac{n\nu}{\bar{\nu}}\right) + \Psi_1(n+1) - 2n\Psi_2(n) - 1 + \gamma_E + \frac{2}{n} \right) \right], \quad (21)$$

where $a_1 = 31C_A/9 - 20T_F n_l/9$. Furthermore, the second line of Eq. (20) results from the second term in square brackets in Eq. (19) after average over the Coulomb wave function.

By expanding the resummed expression up to $\mathcal{O}(\alpha_s^2)$, we get

$$\begin{aligned}
E_{n,\text{hfs}}^{NLL} = & -\frac{16}{3} \frac{C_F^2 \alpha_s^2}{n} \frac{m_r^2}{m_1 m_2} E_n^C \left\{ 1 + \frac{\alpha_s}{\pi} \left[C_F + \frac{7 C_A L_{\alpha_s}^n}{4} + \frac{7 C_A}{8} \ln \left(\frac{4 m_r^2}{m_1 m_2} \right) \right. \right. \\
& + \left(\frac{-3 C_F m_r}{m_1 - m_2} + \frac{3 C_A (m_1 + m_2)}{8 (m_1 - m_2)} \right) \ln \left(\frac{m_1}{m_2} \right) + \frac{n_f T_F (-15 - 11 n + 12 n^2 \Psi_2(n))}{9 n} \\
& \left. \left. - \frac{C_A (-393 - 41 n - 126 \gamma_E n - 126 n \Psi_1(n) + 264 n^2 \Psi_2(n))}{72 n} \right] \right. \\
& + \frac{\alpha_s^2}{\pi^2} L_{\alpha_s}^n \left[L_{\alpha_s}^n \left(\frac{19 C_A^2}{6} - \frac{5 C_A n_f T_F}{6} \right) \right. \\
& + \left(\frac{-C_A^2}{6} - \frac{11 C_A C_F}{8} - \frac{C_F^2 (m_1^2 + m_2^2)}{(m_1 + m_2)^2} \right) \pi^2 - \frac{2 C_F n_f T_F}{3} \\
& + \left(\frac{11 C_A^2 (m_1 + m_2)}{8 (m_1 - m_2)} + \frac{4 C_F n_f T_F m_r}{m_1 - m_2} + C_A \left(\frac{-11 C_F m_r}{m_1 - m_2} \right. \right. \\
& \left. \left. - \frac{n_f T_F (m_1 + m_2)}{2 (m_1 - m_2)} \right) \right) \ln \left(\frac{m_1}{m_2} \right) + \left(\frac{19 C_A^2}{6} - \frac{5 C_A n_f T_F}{6} \right) \ln \left(\frac{4 m_r^2}{m_1 m_2} \right) \\
& \left. \left. - \frac{C_A^2 (-1380 - 305 n - 450 \gamma_E n - 450 n \Psi_1(n) + 924 n^2 \Psi_2(n))}{144 n} \right] \right. \\
& + C_A \left(\frac{43 C_F}{12} + \frac{n_f T_F (-114 - 109 n - 18 \gamma_E n - 18 n \Psi_1(n) + 84 n^2 \Psi_2(n))}{36 n} \right) \right\}, \quad (22)
\end{aligned}$$

where $\alpha_s \equiv \alpha_s(\nu)$, $\Psi_n(x) = d^n \ln \Gamma(x)/dx^n$, $L_{\alpha_s}^n = \ln(C_F \alpha_s/n)$ and $\nu_h = 2m_r$ and $\nu = \bar{\nu}/n$ has been chosen. The $\mathcal{O}(\alpha_s^2 \ln^2 \alpha_s)$ term is known [12, 13], while the $\mathcal{O}(\alpha_s^2 \ln \alpha_s)$ term is new. The equal-mass case expression [9], relevant for charmonium and bottomonium, can be deduced from Eq. (20) by replacing

$$\left(D_{S^2,s}^{(2)} \right)_{\text{1-loop}} \rightarrow \left(D_{S^2,s}^{(2)} \right)_{\text{1-loop}}^{q\bar{q}} \quad (23)$$

and setting $m_1 = m_2$. After including the one-photon annihilation contribution, the Abelian part of the equal-mass result reproduces the $\mathcal{O}(m \alpha_s^6 \ln \alpha_s)$ and $\mathcal{O}(m \alpha_s^7 \ln^2 \alpha_s)$ corrections to the positronium HFS (see *e.g.* [23, 18]).

4 Numerical estimates and conclusions

For the numerical estimates, we adopt the strategy of [9] and replace the on-shell mass of the charm and bottom quarks by one half of the physical masses of the ground state of bottomonium and charmonium [26]. In practice, we take $m_b = 4.73$ GeV and $m_c = 1.5$ GeV, consistent with the accuracy of our computation. Furthermore, we take $\alpha_s(M_Z)$ as an input and run¹ with four-loop accuracy down to the matching scale ν_h to ensure the best

¹For the running and decoupling of α_s we use the program `RunDec` [27].

precision. Below the matching scale the running of α_s is used according to the logarithmic precision of the calculation in order not to include next-to-next-to-leading logarithms in our analysis. In Fig. 1, the HFS for the charm-bottom quarkonium ground state is plotted as a function of ν in the LO, NLO, LL, and NLL approximations for the hard matching scale value $\nu_h = 1.95$ GeV. As we see, the LL curve shows a weaker scale dependence compared to the LO one. The scale dependence of the NLO and NLL expressions is further reduced, and, moreover, the NLL approximation remains stable at the physically motivated scale of the inverse Bohr radius, $C_F \alpha_s m_r \sim 0.9$ GeV, where the fixed-order expansion breaks down. At the scale $\nu' \approx 0.85$ GeV, which is close to the inverse Bohr radius, the NLL correction vanishes. Furthermore, at $\nu'' = 0.92$ GeV, the result becomes independent of ν ; *i.e.*, the NLL curve shows a local maximum corresponding to $E_{\text{hfs}} = 48$ MeV, which we take as the central value of our estimate. The NLL curve also shows an impressive stability with respect to the hard matching scale variation in the physical range $m_c < \nu_h < m_b$, as we observe in Fig. 2. The NLL curve has a local maximum at $\nu_h = 1.95$ GeV, which we take for the numerical estimates. All this suggests a nice convergence of the logarithmic expansion despite the presence of the ultrasoft contribution where α_s is normalized at the rather low scale $\bar{\nu}^2/\nu_h \sim 0.5$ GeV.

Let us discuss the accuracy of our result. For a first estimate of the error due to uncalculated higher-order contributions, we take 6 MeV, the difference of the NLL and LL results at the local maxima. A different estimate can be obtained by varying the normalization scale in the physical range $0.8 \leq \nu \leq 1.4$ GeV. In this case the difference with the maximum is 11 MeV. Being conservative, we take this second number for our estimate of the perturbative error. Within the power counting assumed in this paper, the nonperturbative effects are beyond the accuracy of our computation and should be added to the errors. Following [9], we infer them using charmonium data. For an estimate we attribute the whole difference between perturbation theory and the experimental result, ≈ 14 MeV, to nonperturbative effects. Taking into account that they are suppressed by the heavy quark mass at least as $1/(m_1 m_2 m_r)$, we obtain ≈ 3 MeV for the typical size of the nonperturbative contribution to the HFS in B_c , and take 10 MeV as a conservative estimate of the nonperturbative error.

A further uncertainty is introduced by the error of $\alpha_s(M_Z)$. In Figs. 1 and 2 this is reflected by the yellow band, which is based on $\alpha_s(M_Z) = 0.118 \pm 0.003$. At the scale $\nu'' = 0.92$ GeV it induces an uncertainty of $^{+14}_{-11}$ MeV.

To conclude, we have computed the HFS for a heavy quarkonium composed of quark and antiquark of different flavors in the NLL approximation by summing up the subleading logarithms $\alpha_s^n \ln^{n-1} \alpha_s$ to all orders in the perturbative expansion. The use of the NRG stabilizes the result with respect to the ν variation at the physical scale of the inverse Bohr radius and allow for solid first principle theoretical predictions. An explicit result for the two-loop soft anomalous dimension of the spin-flip potential is also presented.

We predict the mass splitting of the vector and pseudoscalar charm-bottom mesons

$$M(B_c^*) - M(B_c) = 48 \pm 15 \text{ (th)} \begin{array}{l} ^{+14} \\ _{-11} \end{array} (\delta \alpha_s) \text{ MeV} \quad (24)$$

where the errors due to the high-order perturbative corrections and the nonperturbative effects are added up in quadrature in “th”, whereas “ $\delta \alpha_s$ ” stands for the uncertainty in

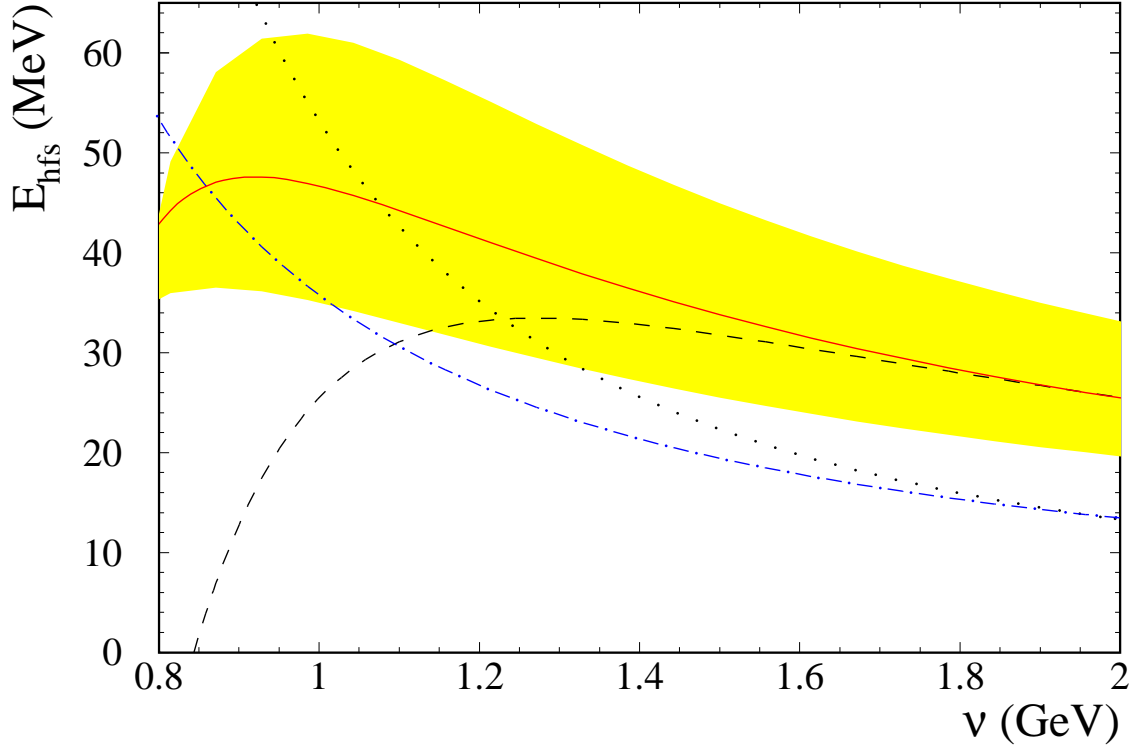


Figure 1: HFS for charm-bottom quarkonium as the function of the renormalization scale ν in LO (dotted line), NLO (dashed line), LL (dot-dashed line), and NLL (solid line) approximation for $\nu_h = 1.95$ GeV. For the NLL result the band reflects the errors due to $\alpha_s(M_Z) = 0.118 \pm 0.003$.

$\alpha_s(M_Z) = 0.118 \pm 0.003$. With improving statistics and precision of the B_c data our result can be considered as a prediction for the B_c^* meson mass.

Acknowledgments:

We thank Bernd Kniehl for carefully reading the manuscript and useful comments. The work of A.A.P. was supported in part by BMBF Grant No. 05HT4VKA/3 and SFB Grant No. TR 9. The work of A.P. was supported in part by MCyT and Feder (Spain), FPA2001-3598, by CIRIT (Catalonia), 2001SGR-00065 and by the EU network EURIDICE, HPRN-CT2002-00311. The work of V.A.S. was supported in part by RFBR Project No. 03-02-17177, Volkswagen Foundation Contract No. I/77788, and DFG Mercator Visiting Professorship No. Ha 202/1. M.S. was supported by HGF Grant No. VH-NH-008.

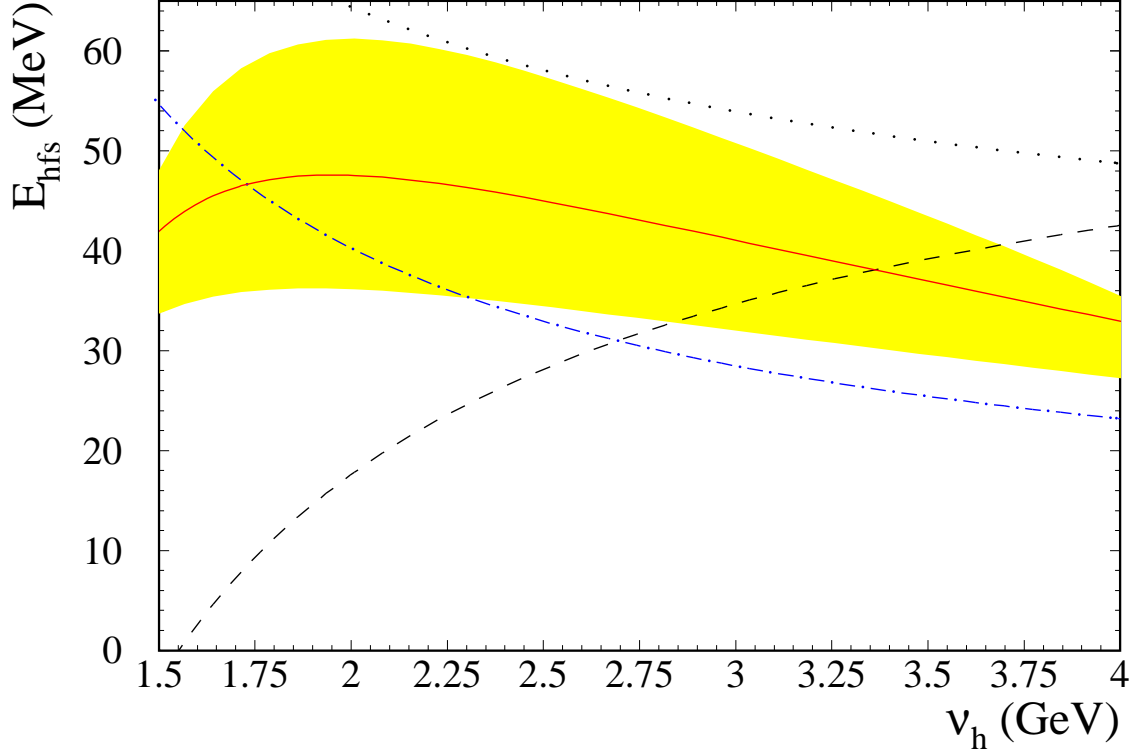


Figure 2: HFS for charm-bottom quarkonium as the function of the hard matching scale ν_h in LO (dotted line), NLO (dashed line), LL (dot-dashed line), and NLL (solid line) approximation for $\nu = 0.95$ GeV. For the NLL result the band reflects the errors due to $\alpha_s(M_Z) = 0.118 \pm 0.003$.

Appendix

The analytical results for the coefficients f_i and A_i of Eq. (14) read ($z = (\alpha_s(\nu_p)/\alpha_s(\nu_h))^{1/\beta_0}$)

$$\begin{aligned}
f_1 &= z^{3\beta_0-2C_A} {}_2F_1\left(3 - \frac{2C_A}{\beta_0}, 1, 4 - \frac{2C_A}{\beta_0}, \frac{z^{\beta_0}}{2}\right), \quad f_2 = z^{2\beta_0-(25C_A)/6}, \\
f_3 &= z^{2\beta_0-4C_A}, \quad f_4 = z^{2\beta_0-3C_A}, \quad f_5 = z^{2\beta_0-2C_A}, \quad f_6 = z^{2\beta_0-2C_A} \ln(2 - z^{\beta_0}), \\
f_7 &= z^{2\beta_0-C_A}, \quad f_8 = z^{\beta_0-(13C_A)/6}, \quad f_9 = z^{\beta_0-2C_A}, \quad f_{10} = z^{\beta_0+C_A}, \\
f_{11} &= z^{2\beta_0}, \quad f_{12} = z^{2\beta_0} \ln(2 - z^{\beta_0}), \quad f_{13} = z^{\beta_0}, \quad f_{14} = z^{\beta_0} \ln(2 - z^{\beta_0}), \\
f_{15} &= z^{3C_A}, \quad f_{16} = \ln(z), \quad f_{17} = 1, \quad f_{18} = \ln(2 - z^{\beta_0}),
\end{aligned} \tag{25}$$

$$\begin{aligned}
A_1 &= \frac{[C_A^2 C_F + 2C_A C_F^2 + \mu_r 4C_F^2(C_A + 2C_F)] (C_A - 8n_l T_F)}{2(5C_A - 4n_l T_F)(9C_A - 4n_l T_F)(2C_A - n_l T_F)}, \\
A_2 &= \frac{[-3456C_A C_F^2 n_l T_F + \mu_r 384C_F^2 n_l T_F(27C_A - 8n_l T_F)] (5C_A + 8C_F)(C_A - 8n_l T_F)}{13C_A(19C_A - 16n_l T_F)(9C_A - 8n_l T_F)(5C_A - 4n_l T_F)(9C_A + 8n_l T_F)}, \\
A_3 &= \frac{-27C_A C_F^2 (C_A - 8n_l T_F)}{8(5C_A - 4n_l T_F)^2(C_A + n_l T_F)} \\
&\quad + \mu_r \frac{3C_F^2(113C_A^3 - 681C_A^2 n_l T_F + 648C_A n_l^2 T_F^2 - 16n_l^3 T_F^3)}{4(5C_A - 4n_l T_F)^3(C_A + n_l T_F)}, \\
A_4 &= \frac{-3C_A C_F}{4(13C_A - 8n_l T_F)}, \\
A_5 &= \frac{27C_F^3 (C_A - 8n_l T_F)(13C_A - 8n_l T_F)}{13(5C_A - 4n_l T_F)(11C_A - 4n_l T_F)(C_A - 2n_l T_F)(2C_A - n_l T_F)} \\
&\quad + \frac{3C_A C_F(11C_A - 16n_l T_F)}{8(5C_A - 4n_l T_F)(2C_A - n_l T_F)} \\
&\quad + \frac{-3C_F^2(6851C_A^3 - 18936C_A^2 n_l T_F + 7968C_A n_l^2 T_F^2 - 832n_l^3 T_F^3)}{208(5C_A - 4n_l T_F)(11C_A - 4n_l T_F)(C_A - 2n_l T_F)(2C_A - n_l T_F)} \\
&\quad + \mu_r \left[\frac{-3C_F^3(481C_A^2 - 346C_A n_l T_F + 64n_l^2 T_F^2)(C_A - 8n_l T_F)}{13C_A(5C_A - 4n_l T_F)(11C_A - 4n_l T_F)(C_A - 2n_l T_F)(2C_A - n_l T_F)} \right. \\
&\quad \left. + \frac{-9C_F^2(39C_A^2 - 284C_A n_l T_F + 88n_l^2 T_F^2)(C_A - 8n_l T_F)}{52(5C_A - 4n_l T_F)(11C_A - 4n_l T_F)(C_A - 2n_l T_F)(2C_A - n_l T_F)} \right], \\
A_6 &= \frac{[3C_A C_F(C_A + 2C_F) + \mu_r 12C_F^2(2C_F + C_A)] (C_A - 8n_l T_F)}{(5C_A - 4n_l T_F)(11C_A - 4n_l T_F)(2C_A - n_l T_F)}, \\
A_7 &= \frac{-3(C_A - 3C_F)C_F}{19C_A - 8n_l T_F}, \\
A_8 &= \frac{[-31104C_A C_F^2 n_l T_F + \mu_r 3456C_F^2 n_l T_F(27C_A - 8n_l T_F)] (5C_A + 8C_F)}{13(9C_A - 8n_l T_F)^2(5C_A - 4n_l T_F)(9C_A + 8n_l T_F)}, \\
A_9 &= \frac{432C_A C_F^3 (C_A - 8n_l T_F)}{(9C_A - 8n_l T_F)(5C_A - 4n_l T_F)^2(11C_A - 4n_l T_F)} \\
&\quad + \frac{-9C_A C_F^2(2481C_A^3 - 1940C_A^2 n_l T_F + 1952C_A n_l^2 T_F^2 - 512n_l^3 T_F^3)}{4(9C_A - 8n_l T_F)(5C_A - 4n_l T_F)^2(11C_A - 4n_l T_F)(C_A + n_l T_F)} \\
&\quad + \mu_r \left[\frac{-72C_F^3(C_A - 8n_l T_F)(21C_A - 8n_l T_F)}{(9C_A - 8n_l T_F)(5C_A - 4n_l T_F)^2(11C_A - 4n_l T_F)} \right. \\
&\quad \left. + \frac{9C_A C_F^2(10401C_A^4 - 24452C_A^3 n_l T_F + 20616C_A^2 n_l^2 T_F^2 - 6240C_A n_l^3 T_F^3 + 256n_l^4 T_F^4)}{(9C_A - 8n_l T_F)(5C_A - 4n_l T_F)^3(11C_A - 4n_l T_F)(C_A + n_l T_F)} \right], \\
A_{10} &= \frac{(-864C_A C_F^3(C_A + n_l T_F) + 27C_A^2 C_F^2(7C_A + 4n_l T_F))(C_A - 8n_l T_F)}{8(5C_A - 4n_l T_F)(C_A - 2n_l T_F)(7C_A - 2n_l T_F)(C_A + n_l T_F)(9C_A + 8n_l T_F)} (1 - 4\mu_r), \\
A_{11} &= \frac{-9C_A^3}{4(11C_A - 4n_l T_F)^2} + \mu_r \frac{3C_F^2}{4(11C_A - 4n_l T_F)},
\end{aligned}$$

$$\begin{aligned}
A_{12} &= \frac{9C_A^3}{2(11C_A - 4n_l T_F)^2}, \\
A_{13} &= \frac{1944C_A C_F^3 (13C_A - 8n_l T_F)}{13(5C_A - 4n_l T_F)(11C_A - 4n_l T_F)^2(C_A - 2n_l T_F)} + \frac{27C_A^2 C_F (3C_A - 4n_l T_F)}{(5C_A - 4n_l T_F)(11C_A - 4n_l T_F)^2} \\
&\quad - \frac{9C_A^3}{(11C_A - 4n_l T_F)^2} - \frac{27C_A C_F^2 (117C_A^2 + 460C_A n_l T_F - 416n_l^2 T_F^2)}{26(5C_A - 4n_l T_F)(11C_A - 4n_l T_F)^2(C_A - 2n_l T_F)} \\
&\quad + \mu_r \left[\frac{-216C_F^3 (585C_A^2 - 554C_A n_l T_F + 64n_l^2 T_F^2)}{13(5C_A - 4n_l T_F)(11C_A - 4n_l T_F)^2(C_A - 2n_l T_F)} \right. \\
&\quad \left. + \frac{-54C_A C_F^2 (325C_A^2 - 1268C_A n_l T_F + 264n_l^2 T_F^2)}{13(5C_A - 4n_l T_F)(11C_A - 4n_l T_F)^2(C_A - 2n_l T_F)} \right], \\
A_{14} &= \frac{216C_A^3 C_F + 432C_A^2 C_F^2}{(5C_A - 4n_l T_F)(11C_A - 4n_l T_F)^2} + \mu_r \frac{1728C_A C_F^3 + 864C_A^2 C_F^2}{(5C_A - 4n_l T_F)(11C_A - 4n_l T_F)^2}, \\
A_{15} &= \frac{-864C_A C_F^3 (C_A + n_l T_F) + 27C_A^2 C_F^2 (7C_A + 4n_l T_F)}{4(5C_A - 4n_l T_F)(C_A - 2n_l T_F)(C_A + n_l T_F)(9C_A + 8n_l T_F)} (1 - 4\mu_r), \\
A_{16} &= \frac{1296C_A^2 C_F^3 + 432C_A^2 C_F^2 (3C_A - n_l T_F)}{(9C_A - 8n_l T_F)(5C_A - 4n_l T_F)(11C_A - 4n_l T_F)} \\
&\quad + \mu_r \frac{-216C_A C_F^3 (21C_A - 8n_l T_F)(5C_A - 4n_l T_F) - 1296C_A^3 C_F^2 (4C_A - 3n_l T_F)}{(9C_A - 8n_l T_F)(5C_A - 4n_l T_F)^2(11C_A - 4n_l T_F)}, \\
A_{17} &= -{}_2F_1 \left(1, 1, 4 - \frac{2C_A}{\beta_0}, -1 \right) \frac{C_F (C_A + 2C_F)(C_A - 8n_l T_F)}{(5C_A - 4n_l T_F)(9C_A - 4n_l T_F)(2C_A - n_l T_F)} (C_A + 4C_F \mu_r) \\
&\quad + \frac{45C_A^3}{4(11C_A - 4n_l T_F)^2} \\
&\quad + \frac{-3C_A C_F}{8(13C_A - 8n_l T_F)(19C_A - 8n_l T_F)(5C_A - 4n_l T_F)(11C_A - 4n_l T_F)^2(2C_A - n_l T_F)} \\
&\quad \times \left(263641C_A^5 - 919114C_A^4 n_l T_F + 1071256C_A^3 n_l^2 T_F^2 - 556448C_A^2 n_l^3 T_F^3 \right. \\
&\quad \left. + 131456C_A n_l^4 T_F^4 - 11264n_l^5 T_F^5 \right) \\
&\quad + \frac{27C_A C_F^3}{(9C_A - 8n_l T_F)^2(19C_A - 16n_l T_F)(5C_A - 4n_l T_F)^2(11C_A - 4n_l T_F)^2} \\
&\quad \times \frac{1}{(7C_A - 2n_l T_F)(2C_A - n_l T_F)} \left(3644181C_A^6 - 7690472C_A^5 n_l T_F + 3453968C_A^4 n_l^2 T_F^2 \right. \\
&\quad \left. + 3026560C_A^3 n_l^3 T_F^3 - 3419648C_A^2 n_l^4 T_F^4 + 1150976C_A n_l^5 T_F^5 - 131072n_l^6 T_F^6 \right) \\
&\quad + \frac{3C_F^2}{16(19C_A - 16n_l T_F)(9C_A - 8n_l T_F)^2(19C_A - 8n_l T_F)(5C_A - 4n_l T_F)^2} \\
&\quad \times \frac{1}{(11C_A - 4n_l T_F)^2(7C_A - 2n_l T_F)(2C_A - n_l T_F)} \left(12488524839C_A^9 \right. \\
&\quad \left. - 37966954860C_A^8 n_l T_F + 37940834480C_A^7 n_l^2 T_F^2 - 1336115840C_A^6 n_l^3 T_F^3 \right. \\
&\quad \left. - 27950404608C_A^5 n_l^4 T_F^4 + 25870953472C_A^4 n_l^5 T_F^5 - 11448205312C_A^3 n_l^6 T_F^6 \right)
\end{aligned}$$

$$\begin{aligned}
& + 2764505088 C_A^2 n_l^7 T_F^7 - 343932928 C_A n_l^8 T_F^8 + 16777216 n_l^9 T_F^9 \Big) \\
& + \mu_r \left[\frac{-3C_F^3}{(19C_A - 16n_l T_F)(9C_A - 8n_l T_F)^2(5C_A - 4n_l T_F)^2(11C_A - 4n_l T_F)^2} \right. \\
& \quad \times \frac{1}{(7C_A - 2n_l T_F)(2C_A - n_l T_F)} (62685009 C_A^7 - 91230606 C_A^6 n_l T_F \\
& \quad - 78455168 C_A^5 n_l^2 T_F^2 + 233772512 C_A^4 n_l^3 T_F^3 - 176816384 C_A^3 n_l^4 T_F^4 \\
& \quad + 58415104 C_A^2 n_l^5 T_F^5 - 7979008 C_A n_l^6 T_F^6 + 262144 n_l^7 T_F^7) \\
& + \frac{-3C_F^2}{4(19C_A - 16n_l T_F)(9C_A - 8n_l T_F)^2(5C_A - 4n_l T_F)^3(11C_A - 4n_l T_F)^2} \\
& \quad \times \frac{1}{(7C_A - 2n_l T_F)(2C_A - n_l T_F)} (659490741 C_A^9 - 1386410130 C_A^8 n_l T_F \\
& \quad - 876382076 C_A^7 n_l^2 T_F^2 + 5528200720 C_A^6 n_l^3 T_F^3 - 7422517824 C_A^5 n_l^4 T_F^4 \\
& \quad + 5156251904 C_A^4 n_l^5 T_F^5 - 2102788096 C_A^3 n_l^6 T_F^6 + 511131648 C_A^2 n_l^7 T_F^7 \\
& \quad \left. - 69730304 C_A n_l^8 T_F^8 + 4194304 n_l^9 T_F^9 \right], \\
A_{18} & = \frac{-18C_A^3(5C_A - 4n_l T_F) - 864C_A^2 C_F^2 - 432C_A^3 C_F}{(5C_A - 4n_l T_F)(11C_A - 4n_l T_F)^2} + \mu_r \frac{-3456C_A C_F^3 - 1728C_A^2 C_F^2}{(5C_A - 4n_l T_F)(11C_A - 4n_l T_F)^2}, \tag{26}
\end{aligned}$$

with $\mu_r = m_r/(m_1 + m_2)$ and ${}_2F_1(a, b; c; z)$ is the hypergeometric function.

References

- [1] CDF Collaboration, F. Abe *et al.*, Phys. Rev. Lett. **81**, 2432 (1998).
- [2] E. J. Eichten and C. Quigg, Phys. Rev. D **49**, 5845 (1994).
- [3] S. S. Gershtein, V. V. Kiselev, A. K. Likhoded and A. V. Tkabladze, Phys. Usp. **38**, 1 (1995) [Usp. Fiz. Nauk **165**, 3 (1995)].
- [4] UKQCD Collaboration, H.P. Shanahan *et al.*, Phys. Lett. B **453**, 289 (1999).
- [5] N. Brambilla and A. Vairo, Phys. Rev. D **62**, 094019 (2000)
- [6] W. Buchmüller, Y.J. Ng, and S.H.H. Tye, Phys. Rev. D **24**, 3003 (1981); S.N. Gupta, S.F. Radford, and W.W. Repko Phys. Rev. D **26**, 3305 (1982); J. Pantaleone, S.H.H. Tye, and Y.J. Ng, Phys. Rev. D **33**, 777 (1986).
- [7] S. Titard and F.J. Yndurain, Phys. Rev. D **49**, 6007 (1994), A. Pineda and F.J. Yndurain, Phys. Rev. D **58**, 094022 (1998); A.A. Penin and A.A. Pivovarov, Nucl. Phys. **B550**, 375 (1999); Yad. Fiz. **64**, 323 (2001) [Phys. Atom. Nucl. **64**, 275 (2001)]; S. Recksiegel and Y. Sumino, Phys. Lett. B **578**, 369 (2004).

- [8] A.A. Penin and M. Steinhauser, Phys. Lett. B **538**, 335 (2002).
- [9] B.A. Kniehl, A.A. Penin, A. Pineda, V.A. Smirnov, and M. Steinhauser, Report No. DESY-03-172, TTP-03-40, UB-ECM-PF-03-28, and hep-ph/0312086.
- [10] W.E. Caswell and G.P. Lepage, Phys. Lett. B **167**, 437 (1986); G.T. Bodwin, E. Braaten, and G.P. Lepage, Phys. Rev. D **51**, 1125 (1995); **55**, 5853(E) (1997).
- [11] A. Pineda and J. Soto, Nucl. Phys. B (Proc. Suppl.) **64**, 428 (1998); B.A. Kniehl and A.A. Penin, Nucl. Phys. **B563**, 200 (1999); N. Brambilla, A. Pineda, J. Soto, and A. Vairo, Nucl. Phys. **B566**, 275 (2000).
- [12] A. Pineda, Phys. Rev. D **65**, 074007 (2002); **66**, 054022 (2002).
- [13] A. V. Manohar and I. W. Stewart, Phys. Rev. D **62**, 014033 (2000); A.H. Hoang and I.W. Stewart, Phys. Rev. D **67**, 114020 (2003).
- [14] M. Beneke and V.A. Smirnov, Nucl. Phys. **B522**, 321 (1998); V.A. Smirnov, *Applied Asymptotic Expansions in Momenta and Masses* (Springer-Verlag, Heidelberg, 2001).
- [15] M.E. Luke, A.V. Manohar, and I.Z. Rothstein, Phys. Rev. D **61**, 074025 (2000).
- [16] G. Amorós, M. Beneke, and M. Neubert, Phys. Lett. B **401**, 81 (1997).
- [17] A. Pineda and J. Soto, Phys. Lett. B **420**, 391 (1998); Phys. Rev. D **59**, 016005 (1999).
- [18] A. Czarnecki, K. Melnikov, and A. Yelkhovsky, Phys. Rev. A **59**, 4316 (1999).
- [19] B.A. Kniehl, A.A. Penin, V.A. Smirnov, and M. Steinhauser, Phys. Rev. D **65**, 091503(R) (2002); Nucl. Phys. **B635**, 357 (2002); Phys. Rev. Lett. **90**, 212001 (2003); **91**, 139903(E) (2003).
- [20] P.A. Baikov, Phys. Lett. B **385**, 404 (1996); Nucl. Instrum. Meth. A **389**, 347 (1997); V.A. Smirnov and M. Steinhauser, Nucl. Phys. **B672** 199 (2003).
- [21] B.A. Kniehl and A.A. Penin, Nucl. Phys. **B577**, 197 (2000).
- [22] R.J. Hill, Phys. Rev. Lett. **86**, 3280 (2001); K. Melnikov and A. Yelkhovsky, Phys. Rev. Lett. **86**, 1498 (2001); B.A. Kniehl and A.A. Penin, Phys. Rev. Lett. **85**, 1210 (2000); **85**, 3065(E) (2000); **85**, 5094 (2000).
- [23] K. Pachucki, Phys. Rev. A **56**, 297 (1997).
- [24] A.V. Manohar, Phys. Rev. D **56**, 230 (1997).
- [25] J.H. Kühn, A.A. Penin, and A.A. Pivovarov, Nucl. Phys. **B534**, 356 (1998); A.A. Penin and A.A. Pivovarov, Phys. Lett. B **435**, 413 (1998); Nucl. Phys. **B549**, 217 (1999); K. Melnikov and A. Yelkhovsky, Phys. Rev. D **59**, 114009 (1999).

- [26] K. Hagiwara *et al.*, Phys. Rev. D **66**, 010001 (2002).
- [27] K. G. Chetyrkin, J. H. Kuhn and M. Steinhauser, Comput. Phys. Commun. **133** (2000) 43.